Eleventh International Conference on Computational Fluid Dynamics (ICCFD11), Maui, Hawaii, USA, July 11-15, 2022

ICCFD11-2022-0601

Wake Breakdown in High-Fidelity CFD Simulations of Rotor-in-Hover: New Tools & Insights

Nathan Hariharan
CREATE Tech Ops Director
HPCMP CREATE
Alexandria, VA, USA

Jennifer Abras
CREATE QA SME
HPCMP CREATE QA
Alexandria, VA, USA

Robert Narducci
Boeing Technical Fellow
The Boeing Company
Philadelphia, PA, USA

Corresponding Author: Nathan Hariharan (nathan.s.hariharan.ctr@mail.mil, nathanaarti@gmail.com)

Abstract: Wake breakdown is a well-documented computational phenomenon associated with highly resolved computational hover predictions. As the computational state-of-the-art for hover predictions has progressed, allowing for higher resolution of the rotor wake, the formation of secondary braids in computed helical wake systems has manifested in various forms. The formation of 3D secondary braids between two parallel convecting vortex filaments, under the right conditions, is physical. Recent hi-definition rotor-hover experiments do confirm their presence. However, computed wake breakdown is more pervasive, and the question of whether high-fidelity methods exaggerate the extent of the secondary vortex production has been a topic of research in the past decade. In this paper, we survey the computational ingredients that make up a high-fidelity hover solver and highlight interesting recent developments. Specifically, two technological tools that enhance the understanding of computed hover vortex dynamics & breakdown are discussed: (i) Direct Volume visualization of computed hover wake vortex dynamics and (ii) Machine Learning-Based automated identification of computed wake breakdown. Direct volume rendering provides insights into the wake breakdown vortical interplay. The automation of vortex-breakdown identification using Machine Learning accelerates the process of physics discovery and provides a hover solution quality alerting mechanism for engineering use-cases.

Keywords: Vortex Dynamics, Hover vortex wake, Helical vortex system, 3D vortex breakdown, rotor hover, volume visualization, Machine Learning

1. Introduction:

The helicopter is a versatile aircraft that covers various flight conditions ranging from level to vertical flight and conditions in between. The hover condition, in particular, plays a crucial role in helicopter design. However, it also represents one of the most difficult aerodynamic conditions to predict accurately. The self-induced flow field coupled with the closely interacting tip-vortex wake has, historically, complicated numerical simulation of hover. In the past, the issue was primarily an overly diffusive prediction where the under-resolved tip vortices would rapidly disappear as the wake age increased. As computational resources increased, more grid resolution was thrown at the problem, mitigating but not solving the issue. Current state-of-the-art hover [1] computing platforms such as OVERFLOW and HPCMP CREATE™-AV HELIOS use adaptive mesh refinement (AMR) and high-order numerical strategies to compute several revolutions of the rotor wake accurately. Figure 1 illustrates this technological shift. As the computational power and methodological capabilities became sufficient to capture a large proportion of the helical wake structure, a new problem emerged, especially for hover computations.

As the high-order/AMR solutions are computed for more time steps, secondary vortex structures appear when the pitch of the helical structure (distance between two successive helical vortex strands) becomes small enough relative to the vortex core size. The evolution of the secondary vortical structures is dramatically shown in Figure 2a-g for the computation of a 4-bladed UH-60A rotor in hover [2] as it progresses through multiple revolutions. At the outset of the computation, instabilities are associated with the starting vortex (Figure 2a-b), but these are removed from the solution as the calculation progresses (Figure 2c). Once the starting vortex is shed off of the computational domain, a relatively clean wake exists briefly (Figure 2c), before secondary instability braids eventually return en masse (Figure 2d-h). The secondary vortex braid instabilities also appear in forward-flight cases [3] and maneuvering cases. However, since the overall vortex system is stabilized by an external flow (non-self-induced by the vortex system as in hover), the presence of secondary braids does not substantially affect the overall computation.

2. Instabilities & Dynamics of 3D Helical Vortex System:

A closer look at the secondary braids reveals their structure. Figure 3 focuses on the vorticity iso-surfaces around the braids bridging successive helical-vortex strands of the central wake. The alternating positive/negative braids hooking around the main helical strands transferring energy from large to small is a classic mixing mechanism in shear-layers. Figure 4 reproduces the picture of LES employing Smagorinski sub-scale model simulations from evolving spatial shear-layers [4]. A well-known phenomenon is the axial braids that bridge the primary spanwise oriented shear-layer roll-up structures.

Thus, given the physical/numerical foundations of what is being solved (i.e., helical vortex systems with small vortical pitch), the appearance of the instability braids between closely convecting vortical strands seems correct. However, the appearance of braids with strength/prevalence entirely overwhelming the stability of the main-helical-wake structure, as seen in most of the finely-resolved S-76 (or similar planforms such as the UH-60/TRAM) computations, is difficult to explain. Further examples of such wake breakdown in refined hover calculations [5][6] are shown in Figure 5.

Analytical work done in the early 70s on inviscid helical vortex instabilities by Widnall [7] remains to date the definitive word on the subject of helical vortex instabilities. Widnall had identified three modes of helical vortex instability, long-wave instability, mutual-inductance instability, and shortwave instability. More recently, Walther et al. [8] used vortex methods to numerically simulate the different helical vortex instabilities identified by Widnall. Walther's work uses a single-blade generated single-strand helical system, but the results are instructive as guidance for multi-strand helical systems. The kind of instability seen in S-76 (and similar) simulations is indicative of a combination of mutual-inductance and shortwave instabilities. Typically, these instabilities are known to grow if the ratio of the separation distance between successive helical vortex strands to the vortex core size becomes smaller than a specific cut-off value. The numerical computations may trigger these instabilities in the near-field for several reasons (i.e., computed core size is too large, other numerical errors, etc.). It was also interesting to observe that numerical hover solutions in earlier cylindrical/axially stretched grids (Figure 6) tend not to break down the near-blade helical system [9]. Once again, there could be several reasons: damped wake, grid stretching damping out instabilities, etc.

Recent experimental evidence shows these structures exist in a rotor wake [10]. Figure 7 illustrates one result from this experiment. The "shake-the-box" technique, a time-resolved particle tracking method, captured secondary braids similar to what is seen in the numerical predictions. However, while these measurements have shown the existence of these secondary structures, the degree to which these structures should develop in a hovering rotor wake still needs further analysis. It is generally accepted that the development of vortex soup is incorrect, but the existence of wake breakdown in some form is considered a real phenomenon. It is hoped that advanced experimental techniques such as the shake-the-box method will help guide where this line lies.

3. High Fidelity Computations and Extraction of Vortex Dynamics Information

The AIAA Hover Prediction Workshop (HPW) [11] efforts have substantially furthered the state-of-the-art knowledge of high-fidelity prediction methods. Reference [12] describes in detail the origins and the evolution of the modern-day hover prediction methodologies. Key questions regarding wake breakdown discussed in Reference[12] include:

1. When does the wake break down?
2. What are the dynamics of the 3D vortical breakdown?
3. Do solver, algorithmic, and turbulence treatments affect breakdown?
4. Do gridding strategies affect wake breakdown?
5. Do geometric-treatment strategies such as root-cut out have any impact?
6. Do computational and convergence strategies have any impact?
7. What is the best method to visualize the 3D dynamics of computed helical wake?
8. Does volume rendering provide better insights?
9. What are the engineering impacts of simulations that exhibit vortex breakdown?
10. Spatial-temporal convergence and its effect on breakdown.

Modern computational rotorcraft tools such as the HPCMP CREATE™-AV HELIOS [13] adopt Cartesian AMR strategies in conjunction with high-order methods to accurately resolve the unsteady vortex system of rotorcrafts. A dual-mesh paradigm is usually employed (Figure 8) - with an unstructured/structured/semi-structured strand mesh solution in the near-body and Cartesian meshes in the off-body - using automated overset information exchange as a means of communication. As computing power has increased, so has the ability to resolve fine scales, with the most recent highest-fidelity hover simulations pushing over half-a-billion grid points. Such an enormous wealth of physics data generated also requires the right tools for the researchers to focus on and extract physics structures of interest.

In the course of the HPW, two different tools sets (i) To advance 3D field visualization of fine-scale vortical dynamics (ii) Machine Learning based auto-extraction of physics have been furthered. This paper focuses on recent developments in these areas and describes how these tools have enabled the acceleration of physics discovery.

3.1 Direct Volume Visualization of the Computed Hover Flow Field

The 3D field solutions that are produced by CFD simulations contain a wealth of information. In the past, the ability to capitalize on this information was limited by available visualization resources and technology. Slices and iso-surfaces became typical visualization techniques in the community, and these practices persist today. While these surface data visualization techniques do have value, the compromises made have not been fully appreciated.

If numerical wake breakdown is present in a simulation, the complete dissipation process of the tip vortex must be quantified. How can such a flow process be assessed in a computational simulation? A practical method is to employ visualization tools to quantify when unstructured vortical flow is completely dominant. The presence of overwhelming secondary structures in the visualization of iso-surfaces is not a reliable indicator and is not sufficient to determine this state. However, direct volume rendering, appropriately used, can effectively quantify a state of wake breakdown. Abras and Hariharan [14] have explored the use of direct volume rendering to enhance the understanding of wake vortex dynamics. Direct volume rendering has been around for several decades but is not widely used in the computational fluid dynamic community as a routine post-processing tool. In recent times, due to increased GPU capabilities and ease of availability in standard flow-visualization software, researchers have begun exploiting the advantages of volume visualization to interrogate complex 3D flow fields.

Traditionally, iso-surfaces and slices with or without a temporal component are employed to visualize 3D flowfields. These methods project 3D information onto 2D manifolds, and these 2D manifolds are rendered. Thus, intrinsically, they make compromises on the information conveyed. A traditional iso-surface of vorticity is shown in figure 9 for a hovering rotor wake. These images were used to determine wake breakdown by looking at the prevalence of the secondary structures. The rate of wake breakdown was quantified by looking at a time series of such images. The problem with iso-surfaces is that they are surface data wrapped in three dimensions. The surface is defined by the locations that represent one value of a particular scalar field. In this instance, all regions that have a vorticity magnitude of 0.05 are shown in the image. All other information is blanked out. Contour slices are often employed as an alternative in order to preserve the information lost in the blanking process. The contour plot of vorticity magnitude shown in figure 10 does not blank out any of the vorticity information. Note that in this specific image, the color scale maximum is set to be the same value as the iso-surfaces shown. Thus, all colors below the color scale maximum represent data lost using the iso-surfaces. The wake sheets and much of the secondary structure detail were lost in the iso-surface images. The compromise with slice data is that the wake structure's spatial resolution is now lost. In particular, the braid structures cannot be identified in a slice image as azimuthal slices generally cut through the axes of these structures. Multiple slices shown in three dimensions cannot remedy this compromise sufficiently.

3D volume rendering does not suffer from such "information culling" handicap as the rendering is based on the entire volume information. Figure 11 shows the exact hovering rotor wake visualization but now employs direct volume rendering. This image contains information in three dimensions and plots the entire scalar field instead of just one level. The analyst no longer has to use expertise to imagine the physics needed to fill the missing regions in the slice and iso-surface formats. Figure 12 shows a similar volume-rendered wake at several time instances as the secondary braids develop. The clarity of the vortical dynamics captured in the volume visualization is substantially better than iso-surface-based methods.

Computational strategies such as tip-vortex AMR and blade-tip grids that spin have recently produced a much cleaner wake solution, and it was not entirely clear why[13]. Direct volume rendering flow visualization techniques and adjustments to the scalar field analyzed have enabled a clearer understanding of why specific gridding/solution strategies produce cleaner wakes. The volume visualization techniques have clarified how the main helical strand and the secondary braids interact and evolve. Such insight has led to the identification that these gridding strategies directly impact the resolution of either the tip vortex or the secondary braid structures. By reducing the resolution of either of these structures, the interplay between the tip vortex and the secondary braids is reduced but not eliminated, delaying the wake breakdown process and the evolution of the wake into vortex soup.

The physics behind the evolution of wake breakdown is better understood using volume rendering techniques[14]. The relative strength of both the braid structures and the tip vortices are significant components of numerical wake breakdown, and the interplay of these two components results in vortex soup. Prior grid studies that have been the focus of the research up until now [14] were shown to impact the strength of either the main helical vortex or the secondary braid. This disruption delays the progression of numerical wake breakdown. In addition, the steady-state rotational case has been shown not to exhibit the features indicative of wake breakdown. This indicates that solution convergence likely contributes to wake breakdown in a larger context. The extension of volume rendering to visualization of the shear layer has provided an explicit means to demonstrate a shear layer instability in the system. Figure 13 shows a 3D volume rendering of the shear layer instabilities.

The application of volume rendering to the wake breakdown research has shown a clear benefit of this visualization technology. In a more general sense, visualization techniques that are not limited by human perception will allow for more excellent analysis capability overall because the results are not left with gaps that are filled by the expectations of the analyst. The opacity transfer function [15] is still a variable that the user must set, and some level of expertise helps with this part of the process, but there is a more minor degree of assumption applied to the process in this format. Figure 14 shows the effects of varying the opacity transfer function for targeting specific aspects of the volumetric flowfield.

3.2 Machine Learning-Based Identification of Wake-vortex Breakdown

One of the central motivations in understanding and characterizing wake breakdown was the implications for engineering decision-making based on high-fidelity hover simulations. High-fidelity codes such as OVERFLOW and HELIOS have been used for the analysis of rotorcrafts and rotor blades by several rotorcraft agencies, including leading industry practitioners. For any rotorcraft calculation, the first significant interest is the integrated aerodynamic efficiency of the installed rotor-blade, i.e., installed Figure of Merit (FM). As has been observed by Hariharan et al. [1] in their status overview paper in 2017, even though absolute FM prediction with an accuracy of less than one count variance has still not been reached, relative predictions are within that requirement. Most active rotorcraft practitioners freeze their gridding/solution strategy once they tune it and then evaluate an extensive database of cases of interest to arrive at accurate relative predictions.

Historically, integrated loads tend to be more forgiving of wake vortex dynamics, especially if the near-wake is relatively well preserved. Figure 15 (from Reference [12]) plots the FM convergence for a whole range of grid variations: baseline, AMR, wedge-family (spinning toroidal), and stationary toroidal. The baseline and stationary toroidal cases exhibit more significant wake breakdown, whereas the wedge-family and AMR cases preserve the helical structure better. In general, the FM convergence curves form two clusters, one for the cases that exhibit breakdown and one for those that do not. Nevertheless, after 20 iterations, the time-averaged FM variations are still bounded within one count for all simulations, consistent with previous observations in Reference [1]. Therefore, the impact of computed wake breakdown on time-averaged aerodynamic load calculations is within engineering bounds of acceptability for relative predictions for blades such as S-76. It will be a stretch to generalize the above statement when the analysis extends to active shapes, which hope to manipulate the tip-vortex formulations to improve efficiency. In addition, for transient problems, interactional problems such as vibration predictions due to transient loading, downwash predictions, etc., computed wake breakdown will have a direct influence.

As long as the wake-breakdown happens sufficiently downstream of the rotor, the figure-of-merit calculations are usually accurate enough for engineering purposes. However, when an engineering evaluation requires running thousands of such simulations, it is impossible to manually visualize the wake structure of each simulation to ensure that the wake breakdown does not happen close to the rotor blade. It will be ideal if an automated system can "visualize" and identify that the wake-breakdown happens sufficiently far downstream and flag down specific cases that do not meet the requirements.

Machine Learning is beginning to touch every aspect of our lives. Machine learning refers to a vast class of mathematical, statistical, and optimization methods that can infer useful information from observed data [17]. The neural-inspired Deep Learning networks are a compelling class of methods [18,19]. These methods mimic the fundamental canonical elements of human neuron interaction at its core level and have non-linearity inbuilt into the modeling process. In physics-based modeling, deep-learning networks are gaining traction through several avenues, i.e., infusion of physics into the learning mechanism [20], augmenting predictive modeling [21]. A quick literature search yields an exploding list of applications related to aerospace engineering, in general, and aerodynamics, in particular.

A specific form of deep-learning network known as the Convolutional Neural Network (CNN) [22,23] has been spectacularly successful in vision and image processing. Abras & Hariharan [23] architected a CNN to classify physics in large-scale 3D fluid dynamic simulation result visualization. In the current workflows involving physics-based simulations, human-in-the-loop visualization of results forms a fundamental basis for inferring physics and also assuring the correctness of the computed results. The primary intent of the work[23] was to assess if CNN-based deep-learning networks can effectively classify physics such as vortical systems or flow separations in computational simulation results and aid further automation of the workflow for routine simulations.

Figure 16 (from Reference [23]) shows the CNN architecture to train and predict where vortex breakdown occurs. Details of the training challenges, curation of CFD data feeding the CNN, and methodology variations that impact the accuracy of predictions are discussed in Reference [23]. Figure 17 shows wake patterns generated by blade tip gridding and solver variations. Figure 18 shows the ML prediction of where the breakdown happens for the cases shown in figure 17. The prediction was off for a few borderline cases, but mostly the ML prediction got it correctly. A scanning process subsequently refined the ML prediction method to precisely identity where the tip vortex centers are located. Figure 19 shows the spatial scanning map – similar to what image recognition systems do -and figure 20 shows the identification of vortex centers. The methodology has been further developed (References 25-27) as a physics inference tool to extract vortical information automatically. Such ML tools dramatically reduce the time to extract physics from large-scale computed solutions – such as the hover wake – speeding up the process of scientific discovery from computational investigations.

The ML method was applied to the wake breakdown problem for an S-76 rotor-wake described extensively in prior publications [4]. The two cases selected for comparison are the Cartesian baseline and the rotational-steady cases [see Reference 4 for details]. These two cases represent the “broken down” and “typical” cases used as examples for the prior discussions. The Cartesian baseline represents a case that exhibits classic breakdown and has been used as the baseline throughout the wake breakdown effort. The rotational-steady case represents a case that was run with identical inputs to the baseline, except for the computational frame of reference employed and the use of steady-state equations. These changes were found to eliminate wake breakdown in the solution. Volume rendered images of the broken-down and intact wake cases are shown in Figure 21. While the breakup of the tip vortices identifying wake breakdown is apparent in the image, the extraction of core property information is non-trivial.

The ML method was used to extract the core information for both of these cases. Scatter plots comparing the baseline and rotational results are provided in Figure 22. These plots compare the tip vortex's radial, and vertical trajectory plotted against wake age. For the first 90 degrees of wake age, the trajectories of the two simulations line up closely. As the wake ages further, these trajectories begin to diverge. In the baseline case, the wake is breaking up; this is represented by the scatter seen in the plots as the vortex cores cease to adhere to the ideal vortex core profile and become more indeterminate. The tip vortex maintains its structure in the rotational case, and tip vortex pairing causes the wake trajectory to diverge. The baseline case does not experience tip vortex pairing as a result of the breakdown.

The matching core property information is plotted in Figure 23. In all of these plots, the breakup of the tip vortex in the baseline case is apparent. Such tip-vortex breakdown is represented by the increasing scatter in the data as the wake ages, and the vortex core profiles become increasingly indeterminate. The rotational case maintains a more consistent core profile for the entire wake age range plotted. The data of value for the comparison are closer to the rotor plane; the baseline case still has a coherent tip vortex. In the range of 0-90 degrees of wake age, the peak vorticity magnitude of the baseline case is higher than that of the rotational case. The high peak vorticity represents a higher velocity gradient across the core of the vortex. However, while the core gradient is higher for the rotational case, the peak tangential velocity at the core boundary is approximately the same for both cases. Unsurprisingly, this represents a tighter core radius in the baseline case compared to the rotational one. When the core radius and the tangential velocity are combined to compute the core circulation, the differences are driven by the core radius since the tangential velocity is approximately the same. The broken-down wake has a smaller vortex core with the same peak velocity; thus, it is not as strong as the vortex in the rotational mode case. Around 90 degrees of wake age, the tip vortex interacts with the following blade. In both cases, the characteristics of the blade vortex interaction are similar. After this point, the baseline case rapidly breaks up, and comparing the core properties is not advisable.

4. Conclusions & Future Directions:

In this paper, we reviewed recent technology developments that have enabled advances in our understanding of computational hover helical wake instabilities. Specifically, two technological tools were discussed (i) Direct Volume visualization of computed hover wake vortex dynamics and (ii) Machine Learning-Based automated identification of computed wake breakdown. The formation of 3D secondary braids between two parallel convecting vortex filaments is physical under the right conditions. Recent hi-definition rotor-hover experiments do confirm their presence. However, computed wake breakdown is more pervasive, and whether high-fidelity methods exaggerate the extent of the secondary vortex production has been a topic of research in the past decade. Some conclusions on our understanding of the computed wake breakdown of hover, leveraging the new technologies:

1. Computational strategies such as tip-vortex AMR, blade-tip grids that spin, etc., have produced a much cleaner wake solution recently, and it was not entirely clear why. More advanced direct volume rendering flow visualization techniques and adjustments to the scalar field analyzed have enabled a more precise evaluation of these critical cases. The volume visualization techniques have clarified how the main helical strand and the secondary braids interact and evolve. This has led to the identification that these gridding strategies directly impact the resolution of either the tip vortex or the secondary braid structures. By reducing the resolution of either of these structures, the interplay between the tip vortex and the secondary braids is reduced but not eliminated, delaying the wake breakdown process and the evolution of the wake into vortex soup.
2. From an engineering standpoint, time-averaged integrated parameters such as the figure of merit are bounded within a prediction spread of one count for simulations that are equally well resolved but have different wake-breakdown characteristics. As long as the wake-breakdown happens sufficiently downstream of the rotor, the figure-of-merit calculations are usually accurate enough for engineering purposes. However, when an engineering evaluation requires running thousands of such simulations, it is impossible to manually visualize the wake structure of each simulation to ensure that the wake breakdown does not happen close to the rotor blade. A Convolutional Neural Net based Machine Learning methodology to automatically identify the vertical wake breakdown location has been developed and validated. The automation of vortex-breakdown identification using Machine Learning accelerates the process of physics discovery and provides a hover solution quality alerting mechanism for engineering use-cases. The Machine Learning method has applications beyond identifying wake breakdown and can generalize to physics inference from computational solutions.
3. The above observations and insights from detailed identification and classification of wake breakdown coupled with the results from rotational-mode computations yielding a clean helical wake - indicate that temporal convergence between time steps is possibly a significant factor in the evolution of wake breakdown in unsteady hover computations.

ACKNOWLEDGMENTS

Material presented in this paper is a product of the CREATE (Computational Research and Engineering for Acquisition Tools and Environments) element of the U.S. Department of Defense HPC Modernization Program. In addition, the authors would like to acknowledge the support of the supercomputing resources provided by the HPCMP, in particular, the Air Force Research Lab (AFRL) and the Army Engineer Research and Development Center (ERDC). The blade and hub models, test reports, and standardization guidance provided through the AIAA Hover Prediction workshop (HPW) are also gratefully acknowledged.

REFERENCES

1. Hariharan, N., Narducci, R., Reed, E., and Egolf, A., "AIAA Standardized Hover Simulation: Hover Performance Prediction Status and Outstanding Issues," *55th AIAA Aerospace Sciences Meeting*, Grapevine, TX, January 2017.
2. Hariharan, N., Wissink, A., Steffen, M., and Potsdam, M., "Tip Vortex Field Resolution Using an Adaptive Dual-Mesh Computational Paradigm," *49th AIAA Aerospace Sciences Meeting*, Orlando, FL, January 2011.
3. Potsdam, M., and Jayaraman, B., "UH-60A Rotor Tip Vortex Prediction and Comparison to Full-Scale Wind Tunnel Measurements," *American Helicopter Society 70th Annual Forum*, Montréal, Québec, May 2014.
4. Comte, P., Silvestrini, J., Begou, P., "Streamwise Vortices in Large Eddy Simulation of Mixing Layers," *Physics of Fluids*, Vol. 4, pp. 2761-2778.
5. Jain, R., "Sensitivity Study of High–Fidelity Hover Predictions on the Sikorsky S-76 Rotor," *Journal of Aircraft*, Vol. 55, No. 1, 2018, pp. 78-88.
6. Chaderjian, N., and Buning, P., "High Resolution Navier-Stokes Simulation of Rotor Wakes," *AHS 67th Annual Forum*, Virginia Beach, VA, May 2011.
7. Widnall, S., "The Stability of a Helical Vortex Filament", *Journal of Fluid Mechanics*, Vol. 54, Part 4, 1972, pp. 641-663.
8. Walther, J.H., et al. "A Numerical Study of the Stability of Helical Vortices Using Vortex Methods," *Journal of Physics*, Series 75, 2007, 012034.
9. Narducci, R., "Hover Performance Assessment of Several Tip Shapes using OVERFLOW," AIAA 2015-1243, *AIAA SciTech 53rd Aerospace Sciences Meeting*, Kissimmee, FL, January 2015.
10. Wolf, C., Schwarz, C., Kaufmann, K., Gardner, A., Michaelis, D., Bosbacj, J., Schanz, D., and Schröder, A., "Experimental Study of Secondary Vortex Structures in a Rotor Wake," *45th European Rotorcraft Forum*, Warsaw, Poland, September 2019.
11. AIAA Hover Prediction Workshop (HPW), AIAA HPW | Hover Prediction Workshop | Rotorcraft Hover (aiaa-hpw.org)
12. Hariharan N., Abras J., and Narducci R., "An Overview of Wake Breakdown in High-Fidelity Simulations of Rotor-in-Hover," Vertical Flight Society 76th Annual Forum, Virginia Beach, VA, October 6-8, 2020.
13. Abras J., and Hariharan N., "Comparison of CFD Hover Predictions on the S-76 Rotor," *Journal of Aircraft*, Vol. 55, No. 1, 2017, pp. 12-22.
14. Abras J., Narducci R., and Hariharan N., "Direct Volume Visualization for Deeper Insights on the Physics of 3D Vorticity Dynamics in the Wake of a Hovering Rotor," *59th AIAA Aerospace Sciences Meeting*, Nashville, TN, January, 2021.
15. Bauer A., Abras J., and Hariharan N., "In Situ and Post-Processing Volume Rendering with Cinema," ISAV, Atlanta, GA, November 16, 2020.
16. Abras J., and Hariharan N., "Comparison of CFD Hover Predictions on the S-76 Rotor," *Journal of Aircraft*, Vol. 55, No. 1, 2017, pp. 12-22.
17. Hastie, T., Tibshirani, R., and Friedman, J., "The Elements of Statistical Learning: Data Mining, Inference and Prediction," Springer-Verlag, New York, 2009.
18. Goodfellow, I., Bengio, Y., and Courville, A., "Deep Learning," MIT Press, 2016.
19. Ng, A., "Deep-Learning," deeplearning.ai, 2018.
20. Raissi, M., Perdikaris, P., and Karniadakis, G., "Physics-informed Neural Networks: A deep-learning framework for solving forward and inverse problems involving nonlinear partial differential equations," Journal of Computational Physics, Volume 378, pp 686-707, February 2019.
21. Singh, A., Medida, S., Duraisamy, K., "Machine Learning-augmented Predictive Modeling of Turbulent Separated Flows over Airfoils," AIAA Journal, Volume 55, Number 7, July 2017.
22. LeCun, Y., Bottou, L., Bengio, Y., and Haffner, P., "Gradient based learning applied to document recognition," Proceedings of the IEEE, Volume 86, Issue 11, November 1998.
23. LeCun, Y., Kavukcuoglu, K., and Farabet, C., "Convolutional networks and applications in vision," *IEEE International Symposium on Circuits and Systems*, Paris, France, May/June 2010.
24. Abras J., Hariharan N., "Application of Machine Learning to Automate Flow Physics Identification in Computed Solutions: Hover Rotor Wake Vortex Identification and Breakdown Analysis," 59th AIAA Aerospace Sciences Meeting, Nashville, TN, January 11-15, 2021.
25. Abras, J., and Hariharan, N., "Machine Learning Based Physics Inference from High-Fidelity Solutions: Vortex Core Extraction," 60th AIAA Aerospace Sciences Meeting, San Diego, CA, January 3-7, 2022.
26. Abras, J., and Hariharan, N., "Machine Learning Based Physics Inference from High-Fidelity Solutions: Vortex Classification and Localization," 60th AIAA Aerospace Sciences Meeting, San Diego, CA, January 3-7, 2022.
27. Abras, J., and Hariharan, N., "Automated Inference of Vortex Core Physics of Hovering Rotor Wakes Using Machine Learning Techniques," Vertical Flight Society's 78th Annual Forum & Display, Ft. Worth, TX, May 2022.

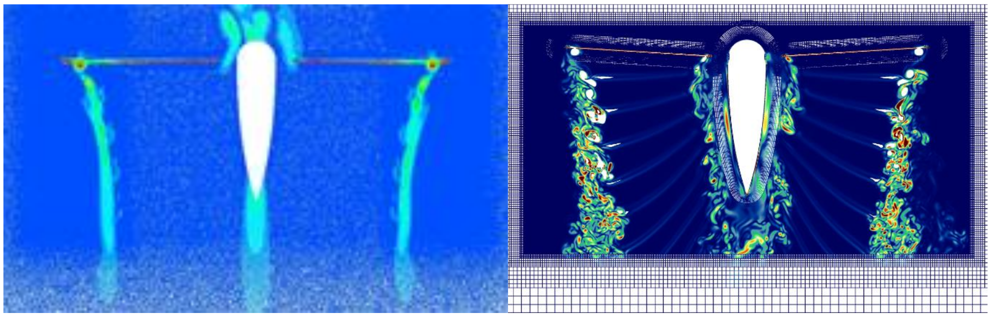

Figure 1. Impact of fully-unstructured vs. higher-order structured computations.

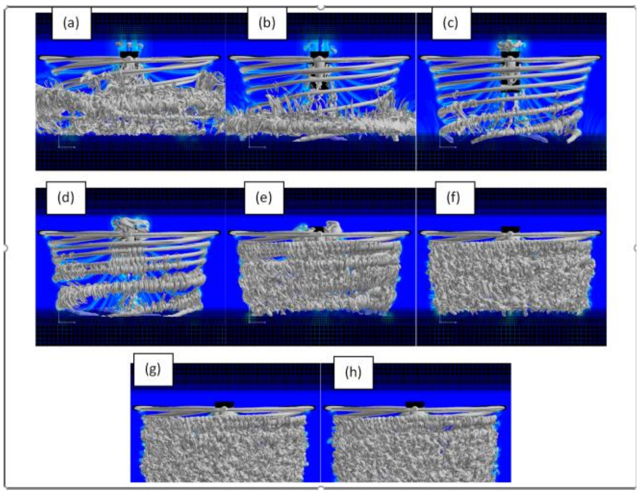

Figure 2. Early manifestations of computed wake instabilities in high-fidelity solutions, from 2011. Computed wake instabilities as the wake evolves for an UH60 blade using Euler off-body solutions, from Reference [2].

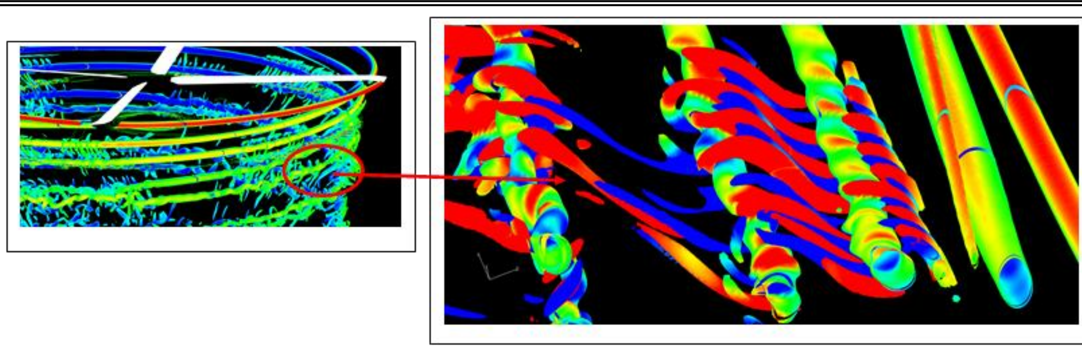

Figure 3. Directional iso-vorticity contours explaining the structure of the secondary vortex generation, similar to shear-layer streamwise hairpin vortex pair generation of alternating rotational orientation.

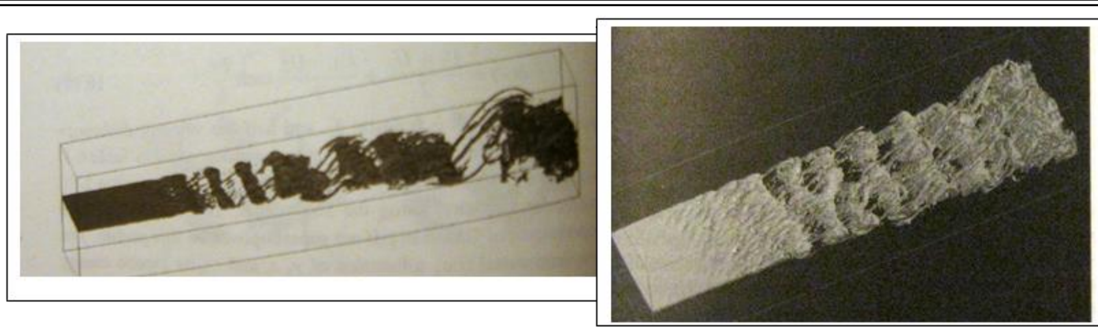

Figure 4. Large eddy simulation of jet shear layer capturing streamwise braids (from Comte et al. [4]).

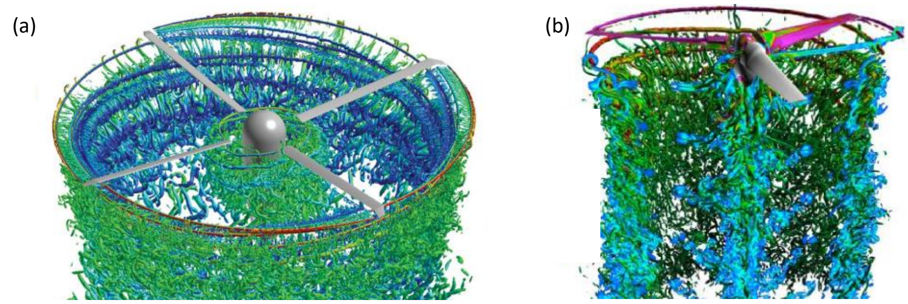

Figure 5. Highly-resolved wake hover simulations (a) 4-bladed S-76 HELIOS simulation with near-body OVERFLOW option (Jain [5]), (b) 3-bladed TRAM OVERFLOW simulation (Chaderjian [6]).

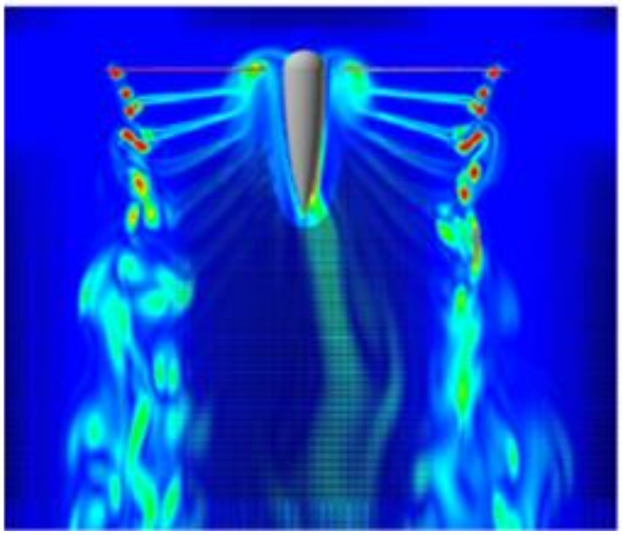

Figure 6. (a) Fig. 6 S-76 OVERFLOW simulation using cylindrical/axially stretched grids, from Narducci [9].

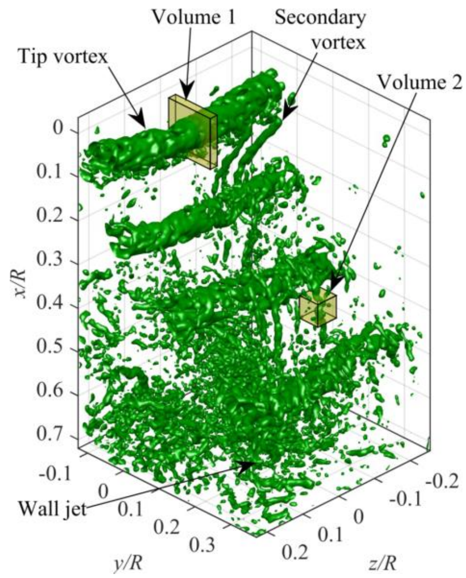

Figure 7. Experimental evidence of secondary vortex structures in a rotor wake, from Wolf et al [10].

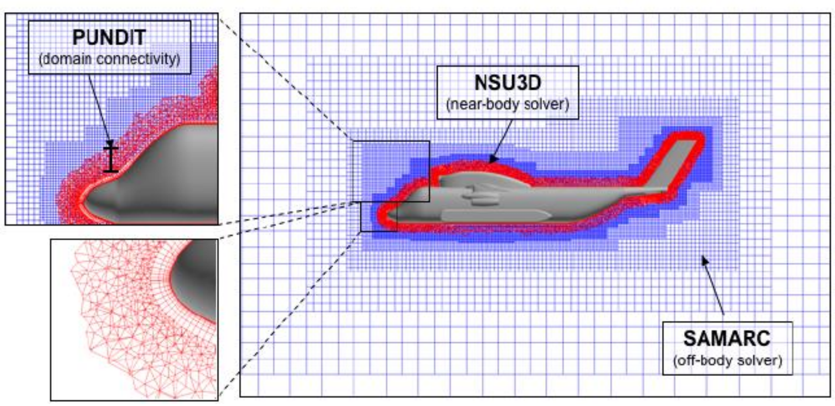

Figure 8. Helios: Dual-mesh paradigm used in the Helios platform with unstructured near-body grids to capture geometric features and boundary layer near the body surface, and block-structured Cartesian grids to capture far-field flow features.

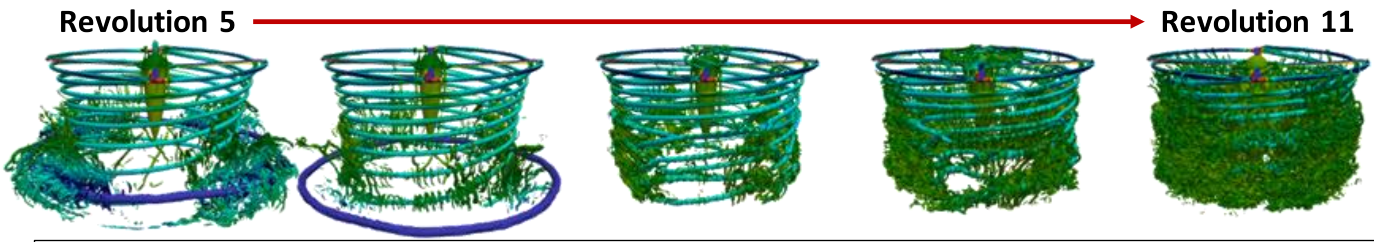

Figure 9: Traditional iso-surface of vorticity plots extracted from the flowfield of a hovering S-76 rotor (from [14])

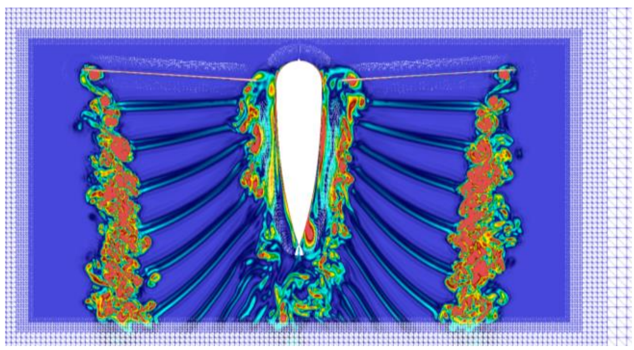

Figure 10: Traditional 2D slice contour plots of vorticity extracted from the flowfield of a hovering S-76 rotor (from [14])

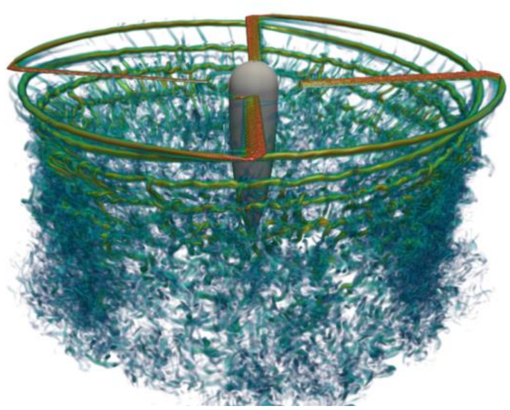

Figure 11: Direct volume rendering of vorticity from the flowfield of a hovering S-76 rotor (from [14])

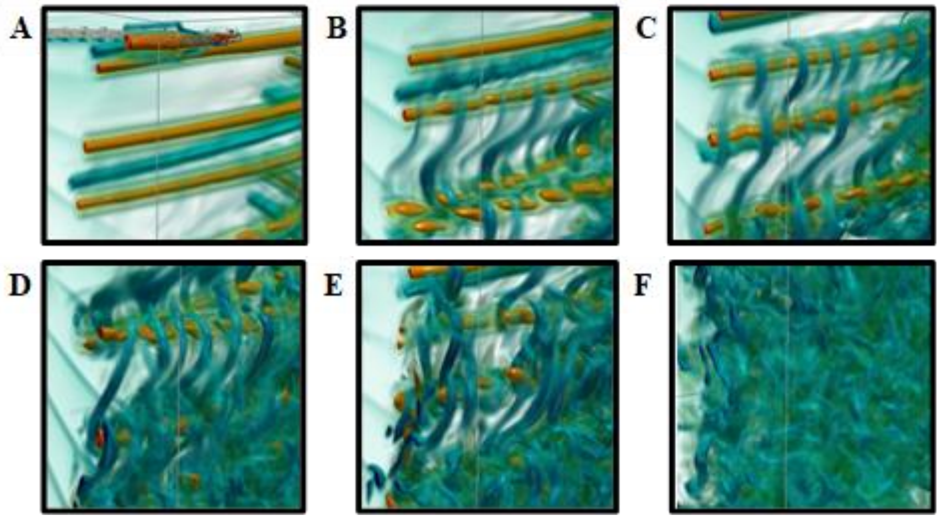

Figure 12. Direct Volume Rendering of computed wake vortex dynamics

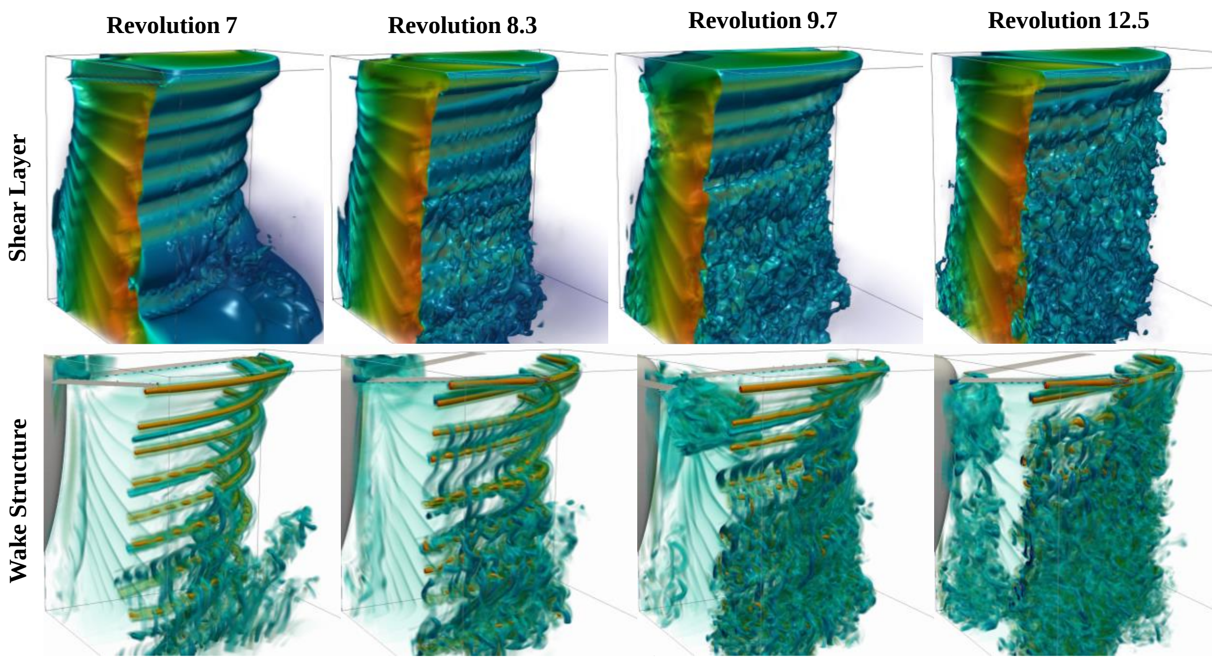

Figure 13: Shear layer evolution (top) and the corresponding wake state (bottom) (from [14])

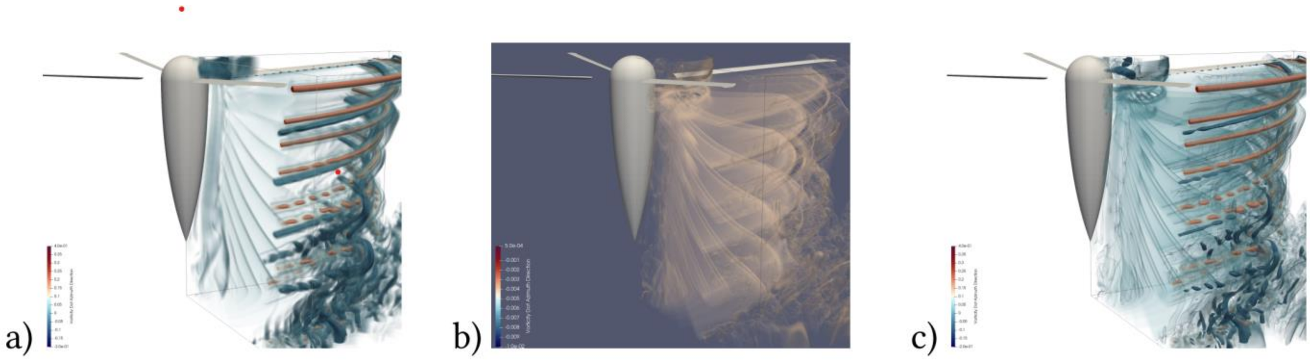

Figure 14: Opacity transfer function variation to target specific physics: (a) Original rendering (b) Targeting wake sheets (c) Combined (from [15])

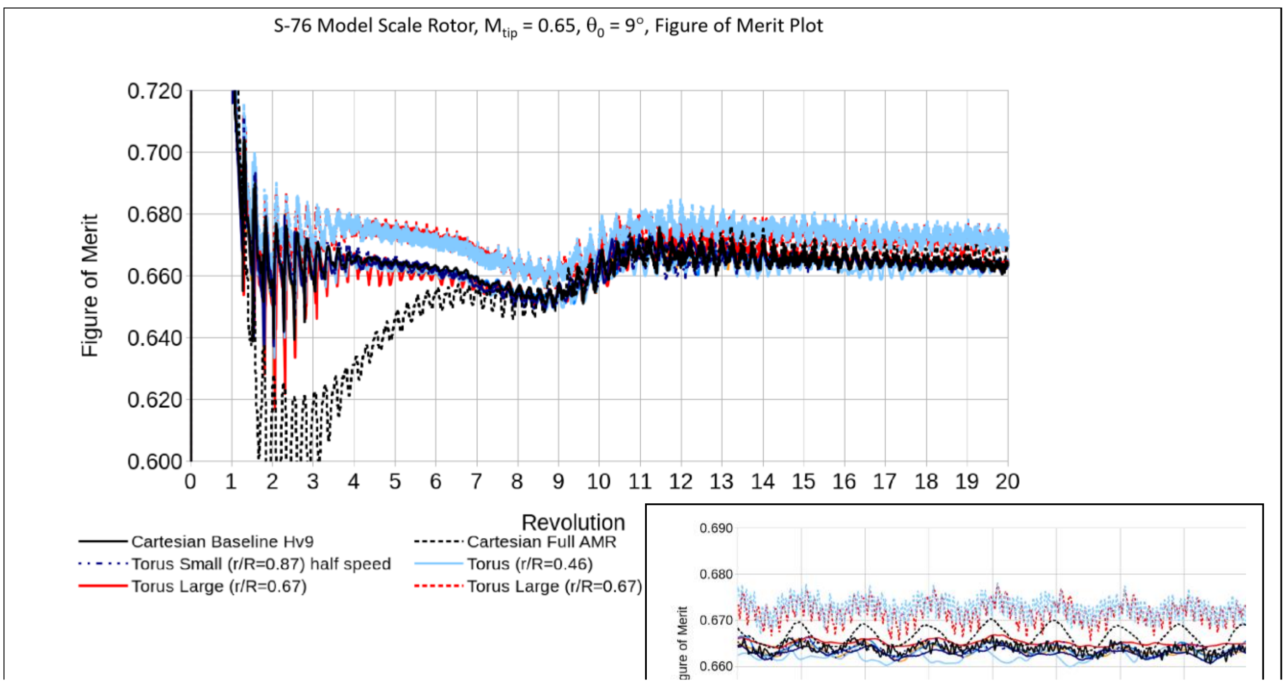

Figure 15: Computed figure of merit calculations for a various gridding strategies.

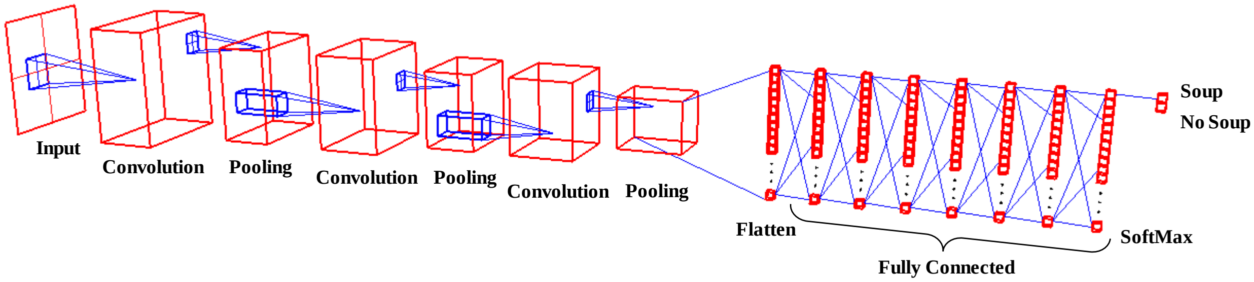

Figure 16: Convolutional Neural Net architecture for vortex breakdown identification.

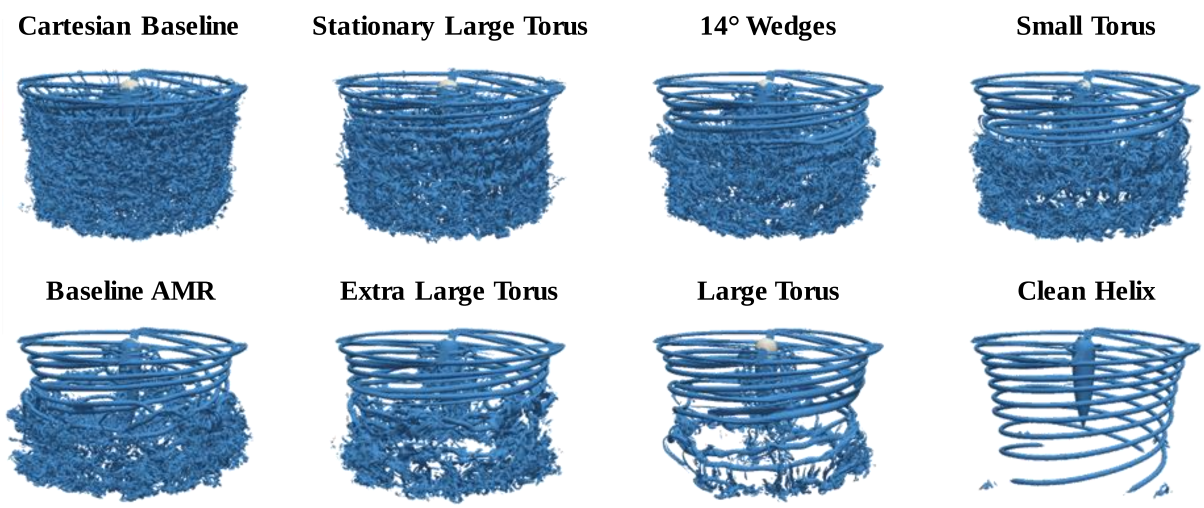

Figure 17: Different wake breakdown patterns generated by various gridding strategies.

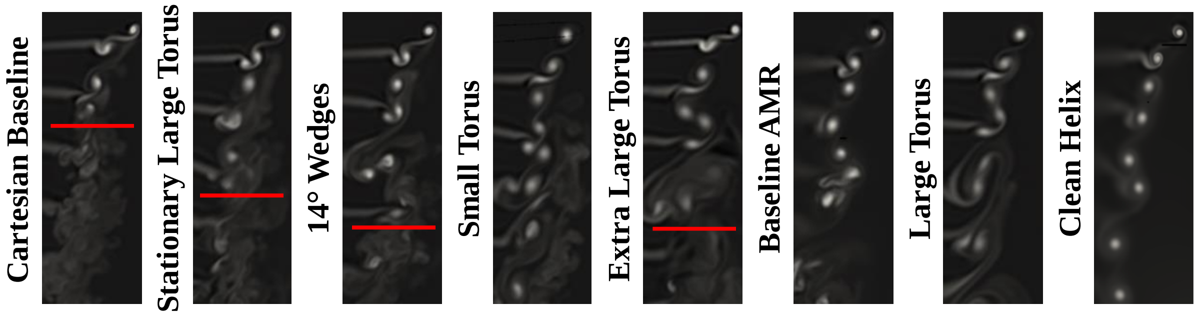

Figure 18: ML identification of the vertical distance from the blade where the breakdown happens.

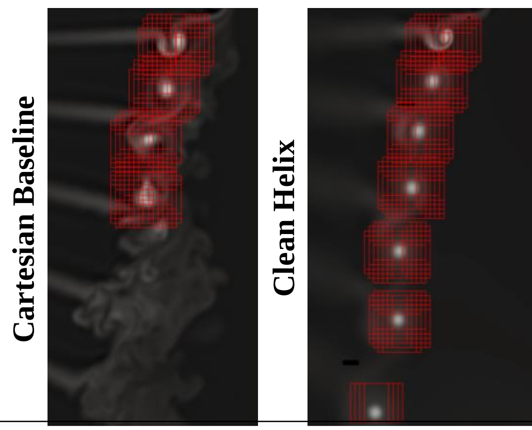

Figure 19: ML methodology variation to identify the location of the vortices.

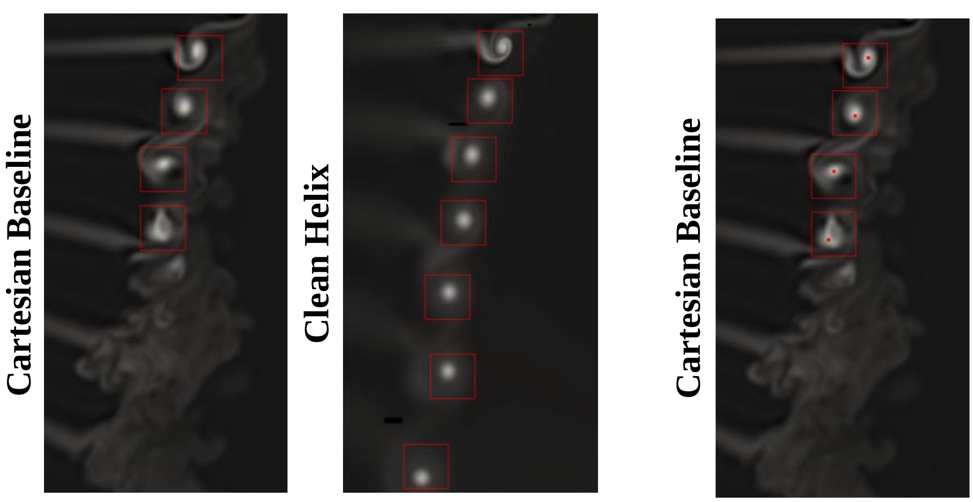

Figure 20: ML methodology identification of tip vortex location.

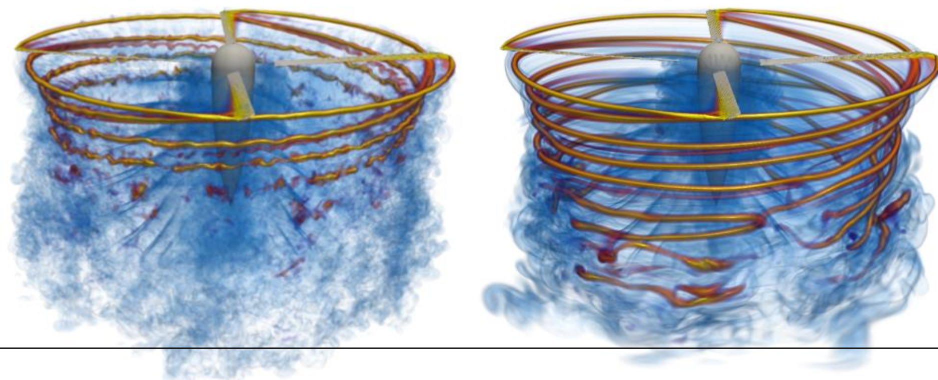

Figure 21: Volume renderings of the Cartesian baseline (left) and rotational steady (right) cases plotting entropy.

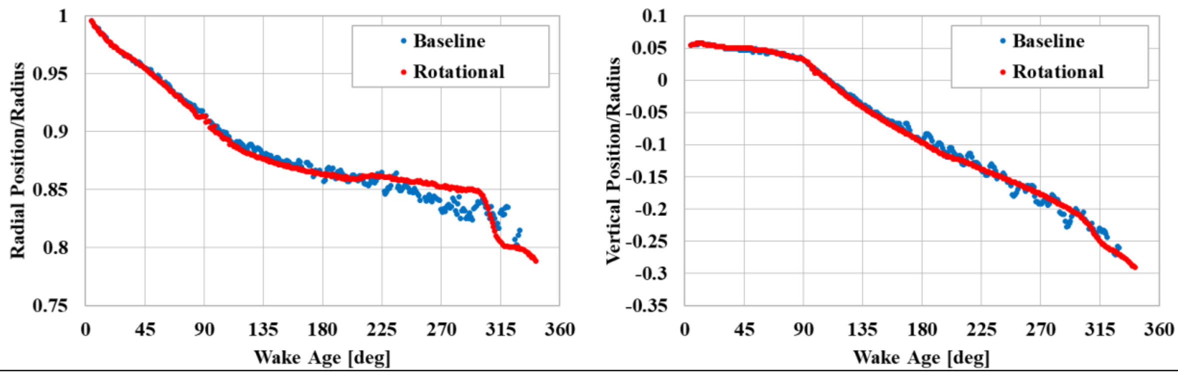

Figure 22: Core trajectory plots comparing the baseline and rotational examples.

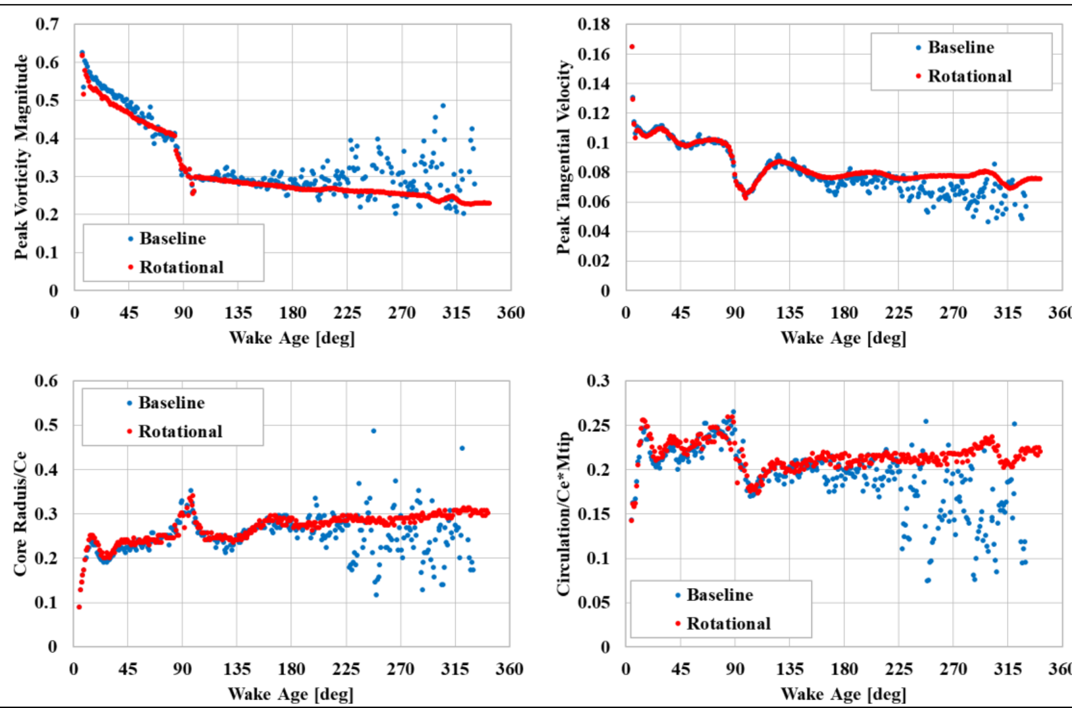

Figure 22: Core property plots comparing the baseline and rotational examples.